PHYSICAL REVIEW D VOLUME 33, NUMBER 7 1 APRIL 1986

Dynamical gluons in low-energy mesons

M. Z. I. Gering and W. D. Heiss
Nuclear Theory Research Group of the Physics Department, University of the Witwatersrand, Johannesburg, South Africa
(Received 15 July 1985; revised manuscript received 26 December 1985)

The meson spectrum below 2000 MeV is calculated within the quark bag model. The frequency dependence of gluon exchanges is explicitly taken into account. Starting from the Bethe-Salpeter equation consistency problems are carefully discussed. Restriction to one-gluon exchange allows the derivation of a Dyson-type equation for the quark-antiquark propagator. Numerical results are in fair agreement with experimental data.

I. INTRODUCTION

Mesons are basically interpreted as quark-antiquark states. The successful description of the gross structure of meson spectroscopy in terms of such states is in fact a cornerstone in support of QCD.[1] When quark confinement is taken into account in a phenomenological way as in the bag model,[2] it appears natural to describe mesons as quark-antiquark states, or in the language of traditional nuclear physics, as particle-hole excitations. This idea of collective excitations should apply even and in particular to the lowest meson—the pion. To view the pion as the Goldstone mode in association with chiral-symmetry breaking from confinement[3] is attractive; from the microscopic point of view this only underlines the collective nature of the pion.[4]

In contrast with nuclear physics, where the nuclear forces can in most cases be successfully approximated by static terms, this approach does not seem to be obvious in the quark bag model. There it is the gluon exchange which is the basic quark-quark interaction as dictated by QCD. Since the lowest gluon modes mingle nicely with the first quark levels in the bag, a static approximation for the quark-quark interaction could be doubtful. In fact, an appreciable admixture of gluon components in all hadrons has been claimed by other authors.[5]

This paper is motivated by the dynamical treatment of the gluons, i.e., by the correct treatment of the frequency dependence of the quark-antiquark interaction. In other words, in addition to the quark-antiquark components of the wave function we explicitly incorporate quark-antiquark-gluon components into the Fock space. Such hybrid states have been discussed in the literature in a perturbative way[6] and it has been stated in the quoted paper that a perturbative treatment is inadequate if the unperturbed $q\bar{q}$ energies are close to or interlacing with the unperturbed $q\bar{q}g$ energies. In this case, a proper diagonalization in the space spanned by $q\bar{q}$ and $q\bar{q}g$ is required. This is exactly what is done in our paper. As a consequence, we get more states and an appreciable mixture of gluonic content into the wave function, in particular, for the higher-lying mesons. Since we begin with the Bethe-Salpeter (BS) equation and employ the Green's-function formalism, only the $q\bar{q}$ projections of the meson states are directly obtained from the residues of the Green's function. The gluonic content can then be determined from the normalization of the states.

The Bethe-Salpeter equation appears to be the appropriate framework whenever a frequency-dependent interaction is to be considered in an interacting many-body system. As the assumption of a bag is made *a priori*, the convenient infinite-momentum frame[7] cannot be used and the BS equation therefore bears all its well-known intricate difficulties. Within the context of our approach these difficulties are carefully discussed in Sec. II. One important aspect is the consistency of a dynamic interaction (the gluon) with the dressing of the single-particle propagators (the quarks). For pragmatic reasons a Dyson-type equation for the quark-antiquark propagator would be desirable rather than the clumsy (but correct) BS equation. A derivation of a Dyson equation under specific assumptions which are pertinent to our approach is presented in Sec. II.

The self-energy (to lowest order) is crucial for theoretical reasons, and this is confirmed by our numerical results. The problems related to the self-energy are discussed in Sec. III. While the expression as such is infinite, we do not embark on a renormalization program but rather use an *ad hoc* cutoff procedure. Arguments are given for justifying this procedure, but a rigorous treatment of this unsatisfactory problem is still outstanding.

In Sec. IV results are presented. Three parameters are used to fit the observed masses of the pion, the ρ, and kaon; these are the bag radius, the coupling constant, and the mass of the strange quark. The higher-lying meson states are then obtained in fair agreement with the experiment, the discrepancy being never greater than 20%. From the wave functions it is obvious that the gluon components are appreciable, and the role of the self-energy is essential in that no reasonable agreement can be obtained by simply ignoring it. By the *a priori* assumption of a bag the principle of a partially conserved axial-vector current cannot hold, yet the pion-decay constant can be computed from $\langle 0 \mid A_\mu(x) \mid \pi \rangle$ which can be directly evaluated; we obtain $f_\pi = 84$ MeV to be compared with $f_\pi^{\text{expt}} = 93$ MeV.

The puzzle with the η meson cannot be tackled when only one-gluon exchange is taken into account. An isospin-dependent force requires at least two gluons,

which causes many additional difficulties as discussed in Sec. II. However, these problems can be dealt with, and since our approach looks rather encouraging judging by the results, we expect that an extension of this procedure should shed more light onto the isospin-zero mesons.

II. FORMAL BACKGROUND

The particular time ordering of the four-point function, viz.,

$$F_{31,24}(t)=i\langle 0\,|\,T[a_4^\dagger(t)a_2(t)a_3^\dagger(0)a_1(0)]\,|\,0\rangle \tag{2.1}$$

contains all the information of interest. In fact, its Fourier transform

$$F_{31,24}(\omega)=\sum_{\nu\neq 0}\left[\frac{\langle 0\,|\,a_4^\dagger a_2\,|\,\nu\rangle\langle\nu\,|\,a_3^\dagger a_1\,|\,0\rangle}{\omega-\omega_\nu+i0}-\frac{\langle 0\,|\,a_3^\dagger a_1\,|\,\nu\rangle\langle\nu\,|\,a_4^\dagger a_2\,|\,0\rangle}{\omega+\omega_\nu-i0}\right] \tag{2.2}$$

displays explicitly the excitation spectrum of the system, i.e., the meson spectrum in the quark bag model as well as the respective quark-antiquark components of the wave functions. In general a Dyson equation for F does not exist (Ref. 13) and F should be obtained from the Fourier transform of the more general four-point function $\mathscr{K}(s,t,u)$ via the expression[8]

$$iF_{31,24}(\omega)=\tfrac{1}{2}\int\frac{ds\,du}{(2\pi i)^2}\mathscr{K}_{1234}(s,\omega,u)\,, \tag{2.3}$$

while $\mathscr{K}$ is the solution of the Bethe-Salpeter equation:

$$\mathscr{K}_{1234}(s,\omega,u)=2\pi\delta(u)G_{14}\left[\frac{s-\omega}{2}\right]G_{23}\left[\frac{s+\omega}{2}\right]+\int\frac{dz}{2\pi i}G_{17}\left[\frac{s-\omega+u}{2}\right]G_{53}\left[\frac{s+\omega+u}{2}\right]U_{7658}(z+s,\omega,z+u)\mathscr{K}_{8264}(z+s-u,\omega,z)\,. \tag{2.4}$$

The fully dressed single-particle Green's function is denoted by G, and U stands for the t-channel irreducible vertex part.[9] Although this equation seems to be intractable it has been used for perturbative QCD calculations in an infinite-momentum frame[5] as it then simplifies due to the nonoccurrence of backwards-going diagrams.

Within the bag model we cannot use this trick. While Eq. (2.4) is then not tractable as it stands, we must nevertheless use it as a guideline so as to eventually arrive at a useful equation for F. Several comments are in order. The irreducible vertex part must be approximated. The equation becomes tractable when a static approximation is made; i.e., the frequency dependence of U is ignored. In this case we obtain the random-phase approximation (RPA) for $F(\omega)$ with its advantages (it is tractable) and disadvantages (its reliability is doubtful in the vicinity of the instability point[10,11]). The RPA has in fact been used for calculating the pion in a chiral-bag model,[4] where the emphasis lies on the possible Goldstone-boson nature of the pion.

As we aim at calculating the low-lying mesons an obvious frequency dependence of U is brought about by gluon-exchange diagrams as discussed in Sec. I. The simplest contribution depicted in Fig. 1 yields

$$U_{1234}(s,t,u)=\sum_g\left[\frac{g_{23}g_{41}^*}{u-\omega_g}-\frac{g_{23}^*g_{41}}{u+\omega_g}\right], \tag{2.5}$$

where the precise form of the vertices g is deferred to the Appendix. The energies ω_g are the gluon modes as obtained from the confinement of the gluons inside the bag. Even this simple expression immediately gives rise to complications when inserted into Eq. (2.4). We list here the three major ones as they concern us for making further progress.

To second order Eq. (2.4) generates a contribution corresponding to the diagram in Fig. 2(a) where two gluons propagate simultaneously. The diagram depicted in Fig. 3 is not generated by Eq. (2.4), yet it should be included if we allow the first diagram to occur; it is actually a part of U that must, in addition, be included explicitly. Needless to say that to higher order such treatment is impractical.

Apart from Figs. 2(a) other time orderings of the four vertices occur. As a consequence, the intermediate lines not only relate to the traditional quark-antiquark states with the quark (antiquark) referring to positive- (negative-) energy states, but also to intermediate states for which the individual particles sit both in positive- or

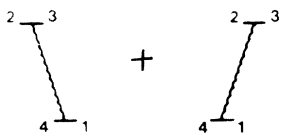

FIG. 1. Simplest nonstatic t-irreducible contribution: a propagating gluon.

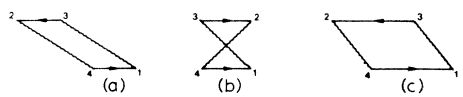

FIG. 2. Second-order contributions generated by Eq. (2.4), i.e., t-reducible contributions.

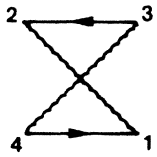

FIG. 3. Second-order t-irreducible contribution that is not generated by Eq. (2.4).

negative-energy states as illustrated in Fig. 2(b). In fact, the correlations invoked by the frequency dependence of U will, for the labels (3,1) and (2,4) in Eq. (2.2), give rise to (pp) and (hh) combinations in addition[8,9] to the usual (ph) and (hp) combinations encountered in the RPA (we use the notation customary in nuclear physics: p for positive- and h for negative-energy states). For illustration a first-order diagram (in U) which contributes to $F_{pp,ph}$ is depicted in Fig. 4.

The third point concerns the dressing of the Green's functions. Consistency problems occur when the dressing is not tuned to the approximation made for the dynamic interaction. For purely forward-going diagrams this mechanism is well understood.[12] If, for instance, only one-gluon exchange is considered at a time [this means to second order that the time of label 3 is before that of label 4 as illustrated in Fig. 2(c)] then the appropriate self-energy is given by Fig. 5(a). If two gluons are admitted at a time [Fig. 2(a)] Fig. 5(b) makes a contribution; likewise, Fig. 3 is associated with Fig. 5(c). We note, however, that the latter cases must also contain vertex corrections in the gluon exchanges; as we confine ourselves to one-gluon exchange in this paper, we do not pursue this aspect further. When backwards-going diagrams must be included, no connection between dressing and interaction has been established to the best of our knowledge. It seems to be plausible and is confirmed to some good extent by our numerical results, that Fig. 5(a) still is the major contribution which must not be left out, if only one gluon at a time is considered. We postpone a discussion of the self-energy [Fig. 5(a)] to Sec. III and focus our attention on the first two points listed above.

Using Eq. (2.5) as input for Eq. (2.4) a solution has been obtained.[9] But the inconsistent treatment of higher-order contributions, such as leaving out the one in Fig. 3, makes this solution unreliable. For our particular problem in mind we omit contributions of more than one gluon at a time; in other words we aim at an infinite series of one-gluon exchanges. Since our intention is the calculation of low-lying meson spectra, we may well, for energy reasons,

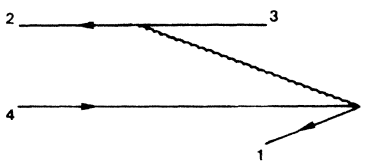

FIG. 4. A contribution to $F_{pp\cdot ph}$. Since the diagram starts with a vacuum process, the actual propagation can begin with both labels 3 and 1 referring to a positive-energy state.

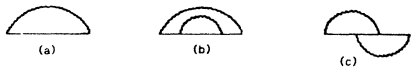

FIG. 5. Self-energy contributions. The particular form of the self-energy that must be included depends on the particular type of gluon-exchange diagrams taken into account.

neglect unperturbed intermediate states containing two gluons. By the same argument, contributions of the kind depicted in Fig. 3 should be excluded; i.e., we restrict our intermediate states to the traditional RPA space (ph) and (hp). These restrictions which characterize specific approximations immediately open the prospects of deriving from Eq. (2.4) a Dyson equation for F, which we denote by a frequency-dependent RPA (Refs. 14 and 15).

Taking for the sake of simplicity the bare Green's function for G and performing the integration as in Eq. (2.3) on the iterated solution of Eq. (2.4) we obtain the series

$$F=F^0+F^0\Delta F^0+F^0\Delta F^0\Delta F^0+\cdots \tag{2.6}$$

as long as we adhere to the restrictions of intermediate states as discussed above.

The calculation yields

$$\Delta^{(\omega)}_{ph,ph}=\sum_g \frac{g_{23}g^*_{41}}{\omega-(\epsilon_3-\delta_4)-\omega_g}+\sum_g \frac{g^*_{23}g_{41}}{\omega-(\epsilon_2-\delta_1)-\omega_g}\,,$$
$$\Delta_{ph,hp}=\sum_g \frac{g_{23}g^*_{41}}{(\epsilon_3-\delta_2)+\omega_g}+\sum_g \frac{g^*_{23}g_{41}}{(\epsilon_4-\delta_1)+\omega_g}\,, \tag{2.7}$$

with ϵ and δ denoting positive- and negative-energy states, respectively; F^0 denotes the familiar free ph propagator known from RPA. Clearly, Eq. (2.6) is the iterative solution of a Dyson equation in RPA space, viz.,

$$F=F^0+F^0\Delta F \tag{2.8}$$

with an effective, frequency-dependent interaction. It is now a simple matter to generalize to the situation where G contains a number of left-hand and right-hand poles owing to dressing. As a consequence, the entry for, say, (ph,ph) with $p\equiv s_{1/2}$ and $h\equiv\bar{s}_{1/2}$ will be fragmented; i.e., the actual matrix will be enlarged, since all the right- (left-) hand poles of $G_{s_{1/2}}$ can combine with all the left- (right-) hand poles of $G_{\bar{s}_{1/2}}$. To bring the enlarged matrix

$$F=[(F^0)^{-1}-\Delta]^{-1} \tag{2.9}$$

into the final form of Eq. (2.2), a sum over the fragmented residues of the poles of F has to be performed.[9]

III. THE SELF-ENERGY

As discussed in Sec. II, the self-energy must be included for reasons of consistency. When the summation over all intermediate gluon and quark states in Fig. 5(a) is performed, the expression diverges logarithmically. Since the bag is a phenomenological model, an attempted renormalization program is not necessarily appropriate. Furthermore, consistency requires the sum to be extended only over those intermediate states that are taken into account in Δ (the gluons) and by the actual space considered in Eq.

(2.9) (the quarks). There remains the question of whether the poles and residues of F depend on the size of the space and the higher-lying gluons. This in turn depends on the behavior of the vertices g_{ik}. If they give rise to a decreasing behavior for higher-lying gluon states and/or higher-lying quark states labeled by i, when k is kept fixed, stable solutions can be expected. Unfortunately, the bag that we use, i.e., the square well which renders the quark and gluon wave functions readily available, does not give rise to a decreasing behavior. The reason is that even the wave functions corresponding to high-lying solutions are confined within the same bag. If the bag had soft boundaries, e.g., $V(r)\sim r^2$, a decreasing behavior of g_{ik} would be the consequence. We, in this work, mimic the soft-bag behavior by multiplying the vertices by a cutoff function chosen to be a Lorentzian in the transferred momentum. Whether, in fact, a soft bag does avoid divergence problems must be subject to more rigorous scrutiny which is not pursued here.

Even when a cutoff is used for the vertices the expression for the self-energy still contains many left- and right-hand poles, thus giving rise to many left- and right-hand poles for the dressed Green's function G. As a consequence, the size of the matrix in Eq. (2.9) becomes very large. Since our interest is focused on the low-lying states, we replace, merely as a numerical device, the more distant poles by a single pole. For the s and p states two right-hand poles and one left-hand pole is sufficient (Table I) while for the higher states only two poles are necessary. Clearly, for the $\bar{s},\bar{p},\bar{d},\ldots$ states right and left must be interchanged.

While we aim at one gluon at a time, we have, by dressing the Green's functions, unavoidably, contributions of two and three simultaneously propagating gluons as illustrated in Fig. 6. This problem can be dealt with consistently for forward-going diagrams,[12,16] but no method is known to us in cases where backwards-going contributions are important. A pragmatic way to suppress this ostensible "overdressing" is to multiply the self-energy by a factor f_Σ. The values listed in Table I are actually obtained for $f_\Sigma=0.2$. The role of this apparent parameter—in fact, a wider range of values for f_Σ is able to produce acceptable results—is discussed in Sec. IV; here we only anticipate that a complete omission of the self-energy, besides being inconsistent, cannot reproduce a satisfactory meson spectrum.

TABLE I. Effective pole positions (first column, in MeV) and residues (second column) of the single-quark Green's functions.

	Light quarks		Strange quarks	
$s_{1/2}$	426	0.809	533	0.819
	1240	0.124	1360	0.126
	−1320	0.051	−1470	0.048
$p_{3/2}$	670	0.607	765	0.644
	1130	0.291	1290	0.287
	−1530	0.073	−1640	0.009
$p_{1/2}$	750	0.761	810	0.838
	1060	0.226	1740	0.137
	−1700	0.010	−1220	0.037
$d_{5/2}$	995	0.936	1080	0.947
	−1490	0.046	−1600	0.037
$d_{3/2}$	1100	0.969	1130	0.966
	−1560	0.007	−1470	0.002

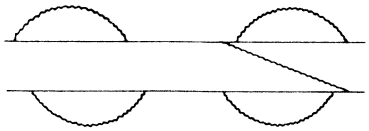

FIG. 6. A diagram illustrating contributions of more than one simultaneous gluon due to dressing.

IV. RESULTS AND DISCUSSION

The wave functions of the quarks and gluons are readily available for the square-well bag. Expressions are given in the Appendix. For convenience the mass of the light quarks has been chosen to be zero.

The vertices g_{ik} can then be calculated. The final expressions for $\Delta(\omega)$ require angular momentum coupling to the total angular momentum of the channel considered, for instance, 0^- for the pion or 1^- for the ρ. The color coupling to a singlet state rules out the quark-antiquark annihilation into one gluon. Final expressions are given in the Appendix.

As a first step in the numerical procedure the self-energy is determined for some values of the bag radius R and coupling constant $\alpha=g^2/4\pi$. The form of the cutoff for the vertices has been chosen as

$$g_{ik}\rightarrow g_{ik}\frac{\Lambda^2}{\Lambda^2+(k_i-k_k)^2+(k_i-k_g)^2+(k_f-k_g)^2}$$

with a suitable value for Λ (850 MeV). This leads to up to 25 poles for the self-energy. For the dressed Green's function the higher-lying poles have been replaced by a single pole for numerical convenience as indicated in Sec. III. Using this fragmented single-particle spectrum the poles and residues of F can be obtained from Eq. (2.9). If the self-energy is not taken into account, the meson spectrum disagrees globally with experimental data in that no fit for R and α could be obtained for which the second 0^- state would lie at least above the first 1^- state, i.e., the ρ. In turn, if the self-energy is not suppressed, the fragmentation of single-particle strength is too strong; as a consequence $\Delta(\omega)$ appears to be weakened to the effect that the splitting between the lowest 0^- and 1^- state, i.e., the pion and the ρ mass, is insufficient. As we argued in Sec. III, a suppressing factor is justified and a good fit can be obtained for $0.1\leq f_\Sigma\leq 0.5$.

The coupling constant is then so determined that the mass ratio between the ρ and the pion agrees with experiment. The bag radius is determined by setting the energy scale. This leads to

$$R=0.92\text{ fm},\quad \alpha=0.76\,,$$

for $f_\Sigma=0.2$ and $\Lambda=850$ MeV. For other choices of f_Σ (in the range indicated) and Λ within 500 MeV

TABLE II. Masses (MeV) of the nonstrange mesons as calculated in this paper.

	Calculated	Observed (Ref. 16)
0^-	139	139 (π)
	1080	1300
	1370	1770
1^-	770	770 (ρ)
	1300	1250
	1600	1600

TABLE III. Masses (MeV) of the strange mesons.

	Calculated	Observed (Ref. 16)
0^-	495	495 (K)
	1250	1400
	1450	1830
1^-	913	892 (K^*)
	1400	1659
	1700	

$\leqq\Lambda\leqq 1200$ MeV, both R and in particular α have to be readjusted to fit the ρ and the pion mass.

Once these parameters are fixed the higher excited states are calculated. The results are listed in Table II and illustrated in Fig. 7. The agreement with available data[17] is remarkably good for the 1^- states and for the 0^- states still within 20%.

A best fit would improve the global pattern, but we did not pursue this approach, since some of these higher-lying states are experimentally doubtful[17] and also theoretically less reliable in our model.

The mass of the strange quark is finally determined to fit the lowest strange meson, i.e., the kaon. With

$$m_s = 220 \text{ MeV}$$

all the strange mesons including the 1^- states are calculated up to 1800 MeV and the results are listed in Table III and Fig. 7. Again the agreement with experiment is fairly good.

Only the quark-antiquark components of the wave functions are obtained from F. They are listed in Table IV. We stress two important features. The Y components (in the traditional RPA notation) are particularly strong for the pion. This indicates that ground-state correlations are brought about essentially by the pion. In this spirit our findings are qualitatively in line with the chiral-bag model where the pion is interpreted as the Goldstone mode.[4] The second important point is the defect of the ph components, i.e., the amount by which $\Sigma\,(X^2-Y^2)$ deviates from unity. For a static RPA this quantity is unity, while in our model the defect indicates the extent of gluon admixtures in the wave function. It is noticeable that these admixtures, albeit globally appreciable, are stronger for the ρ than for the pion. This is expected, since the higher-lying ρ will couple even more strongly to gluons than the lower-lying pion. The importance of gluon admixtures has been noted by other authors.[5]

The knowledge of the matrix elements $\langle 0\,|\,a^\dagger a\,|\,\pi\rangle$ enables us to calculate the pion-decay constant F_π which is defined by the covariant expression[3]

$$\langle 0\,|\,\bar{\psi}(x)\gamma_\mu\gamma_5\psi(x)\,|\,\pi\rangle = \frac{\cos\theta_C k_\mu}{\sqrt{2k_0 V}} F_\pi e^{ikx} \tag{4.1}$$

with k_μ the pion momentum, V the normalization volume, and θ_C the Cabibbo angle. The pion that we have calculated has no sharp momentum, we must rather assume that is has a (spurious) momentum distribution. We therefore have to replace the right-hand side of Eq. (4.1) by a superposition over a range of momenta using a certain distribution function.[18] This is related to the fact that the principle of PCAC (partial conservation of axial-vector current) does not apply here, in that the divergence of the axial-vector current is zero inside and singular at the wall of the bag. Now it turns out that the left-hand

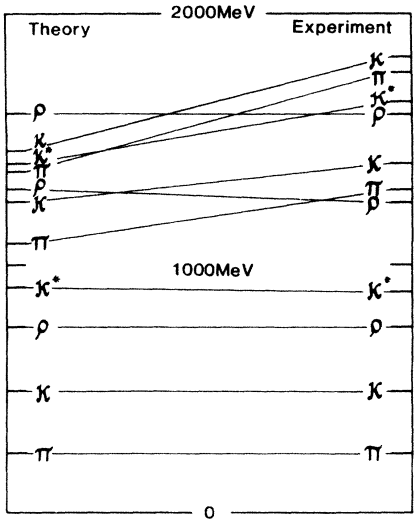

FIG. 7. A diagram which would lift the isospin degeneracy as it can contribute only for $I=0$.

TABLE IV. The quark-antiquark components of the pion and the ρ. X and Y denote the forward- and backward-going parts, respectively.

π	X^2	Y^2	X^2-Y^2
$s_{1/2}\,\bar{s}_{1/2}$	0.823	0.232	0.590
$p_{3/2}\,\bar{p}_{3/2}$	0.599	0.457	0.142
$p_{1/2}\,\bar{p}_{1/2}$	0.005	0.002	0.003
$d_{5/2}\,\bar{d}_{5/2}$	0.287	0.251	0.036
$d_{3/2}\,\bar{d}_{3/2}$	0.001	0.001	0.000
ρ			
$s_{1/2}\,\bar{s}_{1/2}$	0.450	0.003	0.448
$p_{3/2}\,\bar{p}_{3/2}$	0.168	0.027	0.142
$p_{1/2}\,\bar{p}_{1/2}$	0.001	0.000	0.000
$d_{5/2}\,\bar{d}_{5/2}$	0.053	0.025	0.028
$d_{3/2}\,\bar{d}_{3/2}$	0.001	0.000	0.000

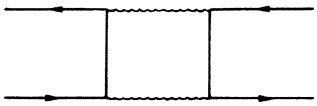

FIG. 8. Comparison of calculated masses with experimental values for low-lying mesons with $J^P=0^-$ and $J^P=1^-$.

side of Eq. (4.1) is weakly dependent on $\mathbf{x}$ thus indicating that the center-of-mass motion of the pion is well peaked around $\mathbf{k}=0$. It is therefore sensible to use Eq. (4.1) at $x=0$ for calculating F_π. We obtain

$$F_\pi = 119 \text{ MeV}$$

to be compared with the experimental value $F_\pi^{\text{expt}}=131$ MeV.

With one-gluon exchange the interaction is isospin independent. It turns out that our results are degenerate with respect to $I=0$ and 1. In particular, in view of the η meson, the experimental facts are different. Isospin-dependent interactions come into the play when two gluons are considered; e.g., the diagram shown in Fig. 8 can only contribute for $I=0$[3]. This indicates that two-gluon effects are important. While they go beyond the scope of this paper, their implications must be carefully considered along the lines discussed in Sec. II.

In view of the strong gluonic admixture that we have found for most mesons except the pion, the question arises whether the incorporation of more gluons renders the $q\bar{q}$ component to a comparatively small part of the mesons. In principle, there is no logical objection against this to happen. But as long as the bag is used as a phenomenological model, caution is required with conclusions that are based on partial summations of particular diagrams.

Finally we turn to meson states with different values for J^P that are observed in the range 1000–2000 MeV. Since we place less credibility on the higher quark states in our model, we do not calculate them as we did the 0^- and 1^- states. We rather estimate these states as being poles of F^0, which, as we recall, are obtained from dressed propagators. Results so obtained are presented and compared with available data in Tables V and VI.

In summary, despite the crudeness of the model a large part of the low-lying meson spectrum can be satisfactorily obtained in this uniform approach. As expected by the nature of the model, the dynamical treatment of the gluons plays a crucial part. Encouraged by our findings, we feel an extension to two gluons is important to tackle the ubiquitous question of the isospin zero states.

TABLE V. Masses of nonstrange mesons with quantum numbers different from those of the pion and ρ family.

	Calculated	Observed
0^+	1180	980
1^+	1080	1190
2^+	1080	1270
2^-	1410	1680
3^-	1340	1670
4^+	1700	2030

TABLE VI. Masses of strange mesons with quantum numbers different from those of the K and K^* family.

	Calculated	Observed
0^+	1300	1350
1^+	1200	1400
2^+	1200	1430
2^-	1500	1580
3^-	1450	1780
4^+	1800	2050

ACKNOWLEDGMENT

The authors gratefully acknowledge discussions with R. H. Lemmer.

APPENDIX

The appropriate boundary conditions for the quark and gluon wave functions, which lead to the unperturbed quark and gluon modes, are given in the literature.[2,19] For the quark spinors we obtain

$$q_n = N_{\nu,\kappa} \begin{bmatrix} ig_{\nu\kappa}(r)\Omega_\kappa^m(\hat{\mathbf{r}}) \\ f_{\nu\kappa}(r)(\boldsymbol{\sigma}\cdot\hat{\mathbf{r}})\Omega_\kappa^m(\hat{\mathbf{r}}) \end{bmatrix},$$

where

$$\Omega_\kappa^m(\hat{\mathbf{r}}) = \sum Y_{lm}^{(\hat{\mathbf{r}})}\chi_\mu(lm_l\tfrac{1}{2}\mu \mid jm),$$

$$g_{\nu\kappa}(r) = j_l(k_{\nu\kappa}r),$$

$$f_{\nu\kappa}(r) = \text{sgn}(\kappa) j_{l'}(k_{\nu\kappa}r).$$

For the longitudinal gluon modes we have

$$a_n^{\mathscr{L}} = N^{\mathscr{L}} j_\Lambda(k_{\mu\Lambda}^{\mathscr{L}}r) Y_{\Lambda M}(\hat{\mathbf{r}}),$$

$$\mathbf{a}_n^{\mathscr{L}} = N^{\mathscr{L}} \frac{\nabla}{k_{\mu\Lambda}^{L}} j_\Lambda(k_{\mu\Lambda}^{\mathscr{L}}r) Y_{\Lambda M}(\hat{\mathbf{r}}),$$

while the transverse magnetic and electric modes read

$$\mathbf{a}_n^{\mathscr{M}} = N^{\mathscr{M}} \frac{\mathbf{L}}{[\Lambda(\Lambda+1)]^{1/2}} j_\Lambda(k_{\mu\Lambda}^{\mathscr{M}}r) Y_{\Lambda M}(\hat{\mathbf{r}}),$$

$$\mathbf{a}_n^{\mathscr{E}} = N^{\mathscr{E}} \frac{\nabla\times\mathbf{L}}{ik_{\mu\Lambda}^{\mathscr{E}}[\Lambda(\Lambda+1)]^{1/2}} j(k_{\mu\Lambda}^{\mathscr{E}}r) Y_{\Lambda M}(\hat{\mathbf{r}}).$$

The vertices

$$g_{ik} = \int d^3r\, \bar{q}_i^c \gamma_\mu \lambda_{cc'}^s q_k^{c'} a^{\mu,s}$$

then factorize[19] into radial integrals, denoted by R_{ik}^g, with g denoting the gluon mode under consideration, a spin angular part of the structure

$$(-1)^{m_f+1/2}\left[\frac{(2j_f+1)(2j_i+1)(2\Lambda+1)}{4\pi}\right]^{1/2}$$
$$\times\begin{pmatrix} j_f & \Lambda & j_i \\ -m_f & M & m_i\end{pmatrix}\begin{pmatrix} j_f & \Lambda & j_i \\ \frac{1}{2} & 0 & -\frac{1}{2}\end{pmatrix},$$

and a color part as indicated by the labels c, c', and s. To obtain the explicit form of the final expressions needed in Eq. (2.7), the respective quark-antiquark pair must be coupled to a total angular momentum J of the meson considered and a color-singlet state. The latter yields a factor $\frac{16}{3}$ from the $\lambda^s\lambda^s$ term which in turn originates from the gluon propagator being diagonal in the color labels. We eventually obtain, for the numerators in Eq. (2.7),

$$(g_{23}g_{41})_J=\frac{16\alpha}{3}R^g_{23}R^g_{41}(-1)^{J+j_1+j_3+l_2+l_4+\Lambda}[(j_1+1)(2j_2+1)(2j_3+1)(2j_4+1)]^{1/2}(2\Lambda+1)$$
$$\times\begin{Bmatrix} j_4 & j_2 & J \\ j_3 & j_1 & \Lambda\end{Bmatrix}\begin{pmatrix} j_1 & \Lambda & j_4 \\ \frac{1}{2} & 0 & -\frac{1}{2}\end{pmatrix}\begin{pmatrix} j_2 & \Lambda & j_3 \\ \frac{1}{2} & 0 & -\frac{1}{2}\end{pmatrix},$$

while isospin yields unity for $I=0$ and $I=1$. Finally, using

$$|\pi\rangle=\sum_{\nu,\kappa}[X_{\nu,\kappa}(a^\dagger b^\dagger)^0_{\nu,\kappa}-Y_{\nu,\kappa}(ab)^0_{\nu,\kappa}]\,|0\rangle\ ,$$

where

$$(a^\dagger b^\dagger)^0_{\nu\kappa}=\sum_m(jmj-m\ |00)a^\dagger_{\nu,\kappa,m}b^\dagger_{\nu,\kappa,m}$$

and

$$\psi(\mathbf{x})=\sum_{\nu,\kappa,m}[q_n(\mathbf{r})a_{\nu,\kappa,m}+\tilde{q}_n(\mathbf{r})b^\dagger_{\nu,\kappa,m}]\ ,$$

where

$$\tilde{q}_n=i\gamma_5\sigma_2 q_n^*\ ,$$

the left-hand side of Eq. (4.1) yields the final expression

$$\langle 0\,|\,\bar{\psi}(\mathbf{x})\gamma_0\gamma_5\psi(\mathbf{x})\,|\,\pi\rangle$$
$$=\sum_{\nu,\kappa}(-1)^l(X_{\nu,\kappa}-Y_{\nu,\kappa})\frac{f_{\nu\kappa}{}^2+g_{\nu\kappa}{}^2}{4\pi}\ .$$

Note that our wave functions carry the dimension $\mathrm{fm}^{-3/2}$. We obtain

$$F_\pi=\left[\frac{8\pi}{3m_\pi}\right]^{1/2}\frac{(Rhc)^{3/2}}{\cos\theta_c}\langle 0\,|\,\bar{\psi}\gamma_0\gamma_5\psi\,|\,\pi\rangle\ .$$

[1] F. E. Close, *An Introduction to Quarks and Partons* (Academic, New York, 1979).

[2] A. Chodos, R. L. Jaffe, K. Johnson, C. B. Thorn, and V. F. Weisskopf, Phys. Rev. D **9**, 3471 (1974); T. DeGrand, R. L. Jaffe, K. Johnson, and J. Kiskis, *ibid.* **12**, 2060 (1975).

[3] T. D. Lee, *Particle Physics and Introduction to Field Theory* (Harwood, Chur, Switzerland, 1981).

[4] V. Bernard, R. Brockmann, M. Schaden, W. Weise, and E. Werner, Nucl. Phys. **A412**, 349 (1984).

[5] S. J. Brodsky, Proceedings of the Fourth Advanced Courses in Theoretical Physics, Stellenbosch, 1985 (unpublished); S. J. Brodsky, in *Short Distance Phenomena in Nuclear Physics,* edited by D. H. Boal and R. M. Woloshyn (Plenum, New York, 1983).

[6] M. Chanowitz and S. Sharpe, Nucl. Phys. **B222**, 211 (1983).

[7] G. P. Lepage, S. J. Brodsky, T. Huang, and P. B. Mackenzie, in *Particles and Fields 2,* edited by A. Z. Capri and A. N. Kamal (Plenum, New York, 1983); J. B. Kogut and D. E. Soper, Phys. Rev. D **1**, 2901 (1970).

[8] C. A. Engelbrecht, F. J. W. Hahne, and W. D. Heiss, Ann. Phys. (N.Y.) **104**, 221 (1977).

[9] W. D. Heiss, C. A. Engelbrecht, and F. J. W. Hahne, Ann. Phys. (N.Y.) **104**, 274 (1977).

[10] M. Z. I. Gering and W. D. Heiss, J. Math. Phys. **25**, 327 (1984).

[11] M. Z. I. Gering and W. D. Heiss, Phys. Rev. C **29**, 1113 (1984).

[12] F. J. W. Hahne, W. D. Heiss, and C. A. Engelbrecht, Phys. Lett. **66B**, 216 (1977).

[13] F. J. W. Hahne and W. D. Heiss, Z. Phys. A **273**, 269 (1975).

[14] C. B. Dover and R. H. Lemmer, Phys. Rev. **165**, 1781 (1968).

[15] M. Z. I. Gering, Ph.D. thesis, Johannesburg, 1985.

[16] W. D. Heiss, C. A. Engelbrecht, and F. J. W. Hahne, Nucl. Phys. **A289**, 386 (1977).

[17] Particle Data Group, Rev. Mod. Phys. **56**, S1 (1984).

[18] J. Donoghue and K. Johnson, Phys. Rev. D **21**, 1975 (1980).

[19] R. D. Viollier, S. A. Chin, and A. K. Kerman, Nucl. Phys. **A407**, 269 (1983).